

Extremely Low Numerical Dispersion FDTD Method Based on H(2, 4) Scheme for Lossy Material

Il-Young Oh¹ · Yongjun Hong² · Jong-Gwan Yook^{1,*}

Abstract

This paper expands a previously proposed optimized higher order (2, 4) finite-difference time-domain scheme (H(2, 4) scheme) for use with lossy material. A low dispersion error is obtained by introducing a weighting factor and two scaling factors. The weighting factor creates isotropic dispersion, and the two scaling factors dramatically reduce the numerical dispersion error at an operating frequency. In addition, the results confirm that the proposed scheme performs better than the H(2, 4) scheme for wideband analysis. Lastly, the validity of the proposed scheme is verified by calculating a scattering problem of a lossy circular dielectric cylinder.

Key Words: Finite-Difference Time-Domain, Higher Order FDTD, Low Dispersion Algorithm, Optimization.

1. Introduction

The finite-difference time-domain (FDTD) method is an elegant way to calculate various electromagnetic phenomena due to its strengths of easy implementation and low computational quantity [1-4]. However, the standard FDTD method (the Yee scheme [5]) has a relatively large number of numerical dispersion errors when compared to other numerical analysis methods, such as the moment method and the finite element method. Many researchers have studied low dispersion algorithms in an attempt to reduce the numerical errors of the standard FDTD method [6-13].

The higher order (2, 4) FDTD scheme (H(2, 4) scheme) is one of the low dispersion FDTD algorithms. Its weakness is that it requires a small time increment to produce accurate results, and even when a small time increment is used, its accuracy is lower than that of other low dispersion FDTD algorithms that use larger time increments at the operating frequency [11, 12]. We previously presented an optimization method for the conventional H(2, 4) scheme [14]. We obtained a high level of accuracy by using the complementary dispersion properties of Yee and the H(2, 4) scheme with propagation angles, which resolved the small time increment problem of the H(2, 4) scheme. This paper expands that solution to a homogeneous, isotropic, and lossy material that has a constant

conductivity for frequencies.

As in our previous study [14], this study uses a weighting factor for isotropic dispersion and two scaling factors in order to achieve an extremely small number of numerical errors. However, unlike the case in the previous study [14], we use a closed-form solution in the present study to find the weighting factor. This study found a weighting factor and two scaling factors under a square grid. Fig. 1

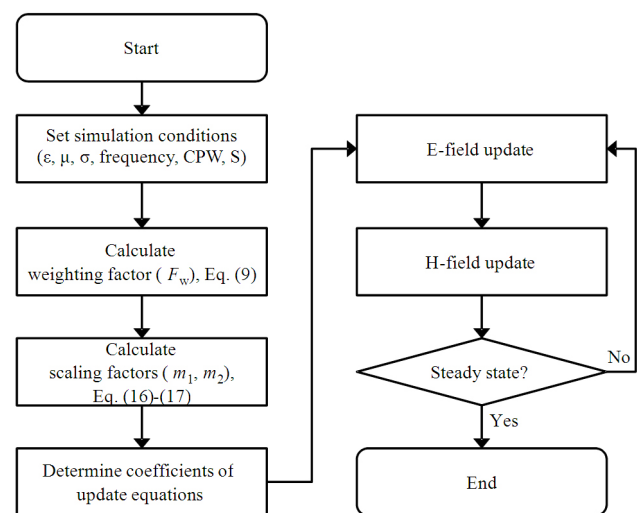


Fig. 1. Flow chart for the proposed scheme. CPW=cells per wavelength, S=Courant number.

Manuscript received March 18, 2013 ; Revised June 20, 2013 ; Accepted July 5, 2013. (ID No. 20130318-008J)

¹School of Electrical and Electronic Engineering, Yonsei University, Seoul, Korea.

²Agency for Defense Development, Daejeon, Korea.

*Corresponding Author : Jong-Gwan Yook (e-mail : jgyook@yonsei.ac.kr)

This is an Open-Access article distributed under the terms of the Creative Commons Attribution Non-Commercial License (<http://creativecommons.org/licenses/by-nc/3.0>) which permits unrestricted non-commercial use, distribution, and reproduction in any medium, provided the original work is properly cited.

shows the procedure of the proposed scheme. Section II presents the formulation of the numerical dispersion relations and the calculation of a new weighting factor by a closed-form solution. The scaling factors are calculated and the scheme's performance is analyzed in Section III. The numerical results of the proposed scheme and the H(2, 4) scheme are compared in Section IV.

II. Formulation

In this section, nearly isotropic numerical phase constants for the propagation angles were obtained using a weighting factor. We assumed a square grid and found the weighting factor by using update equations and a numerical dispersion relation. The Maxwell equations used in the FDTD method are as follows:

$$\nabla \times \bar{E} = -\mu \frac{\partial \bar{H}}{\partial t}, \quad (1)$$

$$\nabla \times \bar{H} = \varepsilon \frac{\partial \bar{E}}{\partial t} + \sigma \bar{E}, \quad (2)$$

where \bar{E} is the electric field intensity and \bar{H} is the magnetic field intensity. In addition, ε , μ , and σ are respectively the permittivity, permeability, and conductivity of a material. The following equations show the update equations of the proposed scheme at TM_z -mode. A square grid ($\Delta = \Delta x = \Delta y$) is assumed.

$$\begin{aligned} H_x^{n+\frac{1}{2}}\left(i, j+\frac{1}{2}\right) &= H_x^{n-\frac{1}{2}}\left(i, j+\frac{1}{2}\right) \\ &- \frac{\Delta t}{\mu \Delta} \left[\left(1 + \frac{F_w}{8}\right) d_y^2 E_z^n\left(i, j+\frac{1}{2}\right) - \frac{F_w}{24} d_y^4 E_z^n\left(i, j+\frac{1}{2}\right) \right], \end{aligned} \quad (3)$$

$$\begin{aligned} H_y^{n+\frac{1}{2}}\left(i+\frac{1}{2}, j\right) &= H_y^{n-\frac{1}{2}}\left(i+\frac{1}{2}, j\right) \\ &+ \frac{\Delta t}{\mu \Delta} \left[\left(1 + \frac{F_w}{8}\right) d_x^2 E_z^n\left(i+\frac{1}{2}, j\right) - \frac{F_w}{24} d_x^4 E_z^n\left(i+\frac{1}{2}, j\right) \right], \end{aligned} \quad (4)$$

$$\begin{aligned} E_z^{n+1}(i, j) &= \frac{2\varepsilon - \sigma \Delta t}{2\varepsilon + \sigma \Delta t} E_z^n(i, j) \\ &+ \frac{2\Delta t}{(2\varepsilon + \sigma \Delta t)\Delta} \left(1 + \frac{F_w}{8}\right) \left\{ d_x^2 H_y^{n+1/2}(i, j) - d_y^2 H_x^{n+1/2}(i, j) \right\} \\ &- \frac{2\Delta t}{(2\varepsilon + \sigma \Delta t)\Delta} \frac{F_w}{24} \left\{ d_x^4 H_y^{n+1/2}(i, j) - d_y^4 H_x^{n+1/2}(i, j) \right\}. \end{aligned} \quad (5)$$

where $d_x^{i=2,4}$ is the difference operator defined as:

$$d_x^2 f(i, j) = f(i+1/2, j) - f(i-1/2, j), \quad (6)$$

$$d_x^4 f(i, j) = f(i+3/2, j) - f(i-3/2, j). \quad (7)$$

F_w is the weighting factor. E and H are the electric intensity and magnetic field intensity, respectively. Their

subscripts indicate the field component direction. Δx and Δy denote the unit cell length of the x-direction and y-direction, respectively. Δt is a time increment. The update equations are composed of the weighting sum of the update equations of the Yee and H(2, 4) schemes. The ratio of the Yee and H(2, 4) schemes is determined by the weighting factor. If the weighting factor is one, the proposed scheme becomes the H(2, 4) scheme, and if the weighting factor is zero, the proposed scheme becomes the Yee scheme.

Eq. (8) is the numerical dispersion relation of the proposed scheme.

$$\begin{aligned} \sin^2\left(\frac{\tilde{k}_x}{2}\right) \left\{ 1 + \frac{F_w}{6} \sin^2\left(\frac{\tilde{k}_x}{2}\right) \right\}^2 &+ \sin^2\left(\frac{\tilde{k}_y}{2}\right) \left\{ 1 + \frac{F_w}{6} \sin^2\left(\frac{\tilde{k}_y}{2}\right) \right\}^2 \\ &= \left(\frac{\Delta}{c\Delta t} \sin\left(\frac{\omega\Delta t}{2}\right) \right)^2 - j \frac{\sigma\mu\Delta}{4\Delta t} \sin(\omega\Delta t). \end{aligned} \quad (8)$$

where $\tilde{k}_x = \tilde{k} \cos \phi$ and $\tilde{k}_y = \tilde{k} \sin \phi$. ϕ is the propagation angle and c is the velocity of light. As shown in Fig. 2, the numerical phase constants of the H(2, 4) scheme and the proposed scheme have similar patterns in the propagation angles. They were obtained by Newton's method [15]. The H(2, 4) and Yee schemes have a maximum numerical phase constant on the main axes and a minimum value on the diagonal axes. However, the phase constants of the Yee scheme are larger than the analytic phase constant, while those of the H(2, 4) scheme are smaller than the analytic value. This property makes the two schemes complementary. If the proposed scheme is used, better isotropic dispersion properties will be obtained than those of the H(2, 4) scheme.

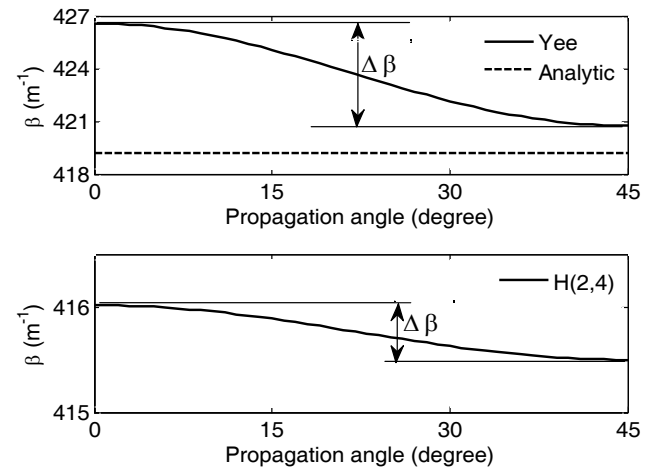


Fig. 2. Numerical phase constants of Yee [5], the H(2, 4) scheme and analytic phase constants. Cells per wavelength are 8 at 10 GHz and the Courant number is 0.6. The relative permittivity and permeability are 4 and 1, respectively. The conductivity is 0.05 S/m.

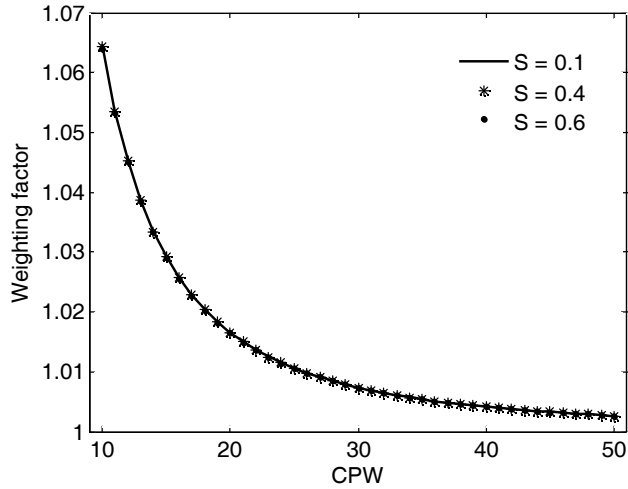


Fig. 3. Weighting factor versus cells per wavelength (CPW) at different Courant numbers (S). The relative permittivity is 4 and the conductivity is 0.05 S/m.

We determined the weighting factor (F_w) using the following equation:

$$F_w \cdot \Delta\beta_H = -(1 - F_w) \cdot \Delta\beta_Y, \quad (9)$$

$$\Delta\beta(\text{CPW}) = \max\{\beta(\phi, \text{CPW})\} - \min\{\beta(\phi, \text{CPW})\}. \quad (10)$$

$\Delta\beta$ is defined by Eq. (10) and the subscript indicates the numerical scheme (H : H(2, 4) and Y : Yee). Eq. (9) flattens the numerical wavenumbers of the proposed scheme for the propagation angles at the operating frequency.

Fig. 3 shows the weighting factor versus cells per wavelength (CPW). As shown in Fig. 3, the Courant number (S) has little effect on the weighting factor. As the CPW become larger, the weighting factor approaches a val-

ue of one. Fig. 4 shows the *flatness* of the relative permittivity and conductivity, defined as follows:

$$\Delta\varepsilon_r(\text{CPW}) = \max\{\varepsilon_r(\phi, \text{CPW})\} - \min\{\varepsilon_r(\phi, \text{CPW})\} \quad (11)$$

$$\Delta\sigma(\text{CPW}) = \max\{\sigma(\phi, \text{CPW})\} - \min\{\sigma(\phi, \text{CPW})\} \quad (12)$$

where $\max(X)$ and $\min(X)$ stand for the maximum and minimum value of X , respectively. As shown in Fig. 4, the proposed scheme clearly has the best performance among the three schemes. Its *flatness* is sufficiently small to consider a constant relative permittivity and conductivity for propagation angles.

III. Numerical Error Reduction

In this section, the numerical errors are removed at a single frequency. This is followed by analysis of the wide band properties. Fig. 5 shows the relative permittivity and conductivity for the propagation angles. The estimated material constants of the proposed scheme (uncorrected) are much flatter than those of the H(2, 4) scheme. However, the difference is greater between the analytic solution and these constants than between those of the H(2, 4) scheme. These numerical errors were reduced by multiplying two scaling factors, m_1 and m_2 , by the relative permittivity and conductivity, respectively. These create a new relative permittivity and conductivity, defined as

$$\varepsilon_{r, \text{new}} = m_1 \times \varepsilon_r, \quad (13)$$

$$\sigma_{\text{new}} = m_2 \times \sigma. \quad (14)$$

These new material constants change the numerical dis-

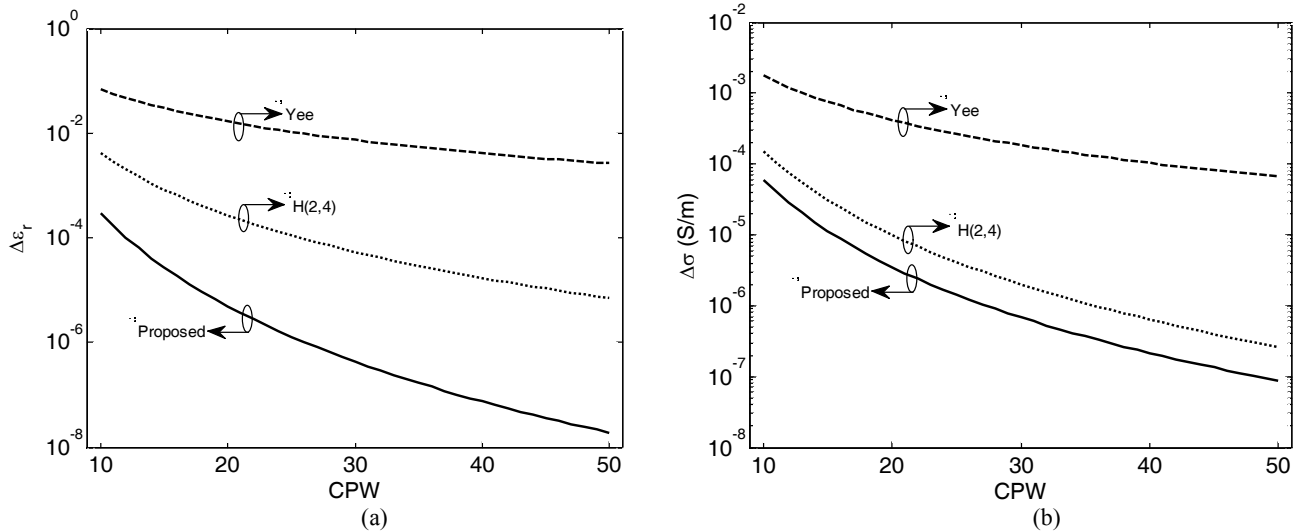


Fig. 4. (a) *flatness* of relative permittivity ($\varepsilon_r=4$) and (b) *flatness* of conductivity ($\sigma=0.05$ S/m) versus cells per wavelength (CPW). The Courant number is 0.6.

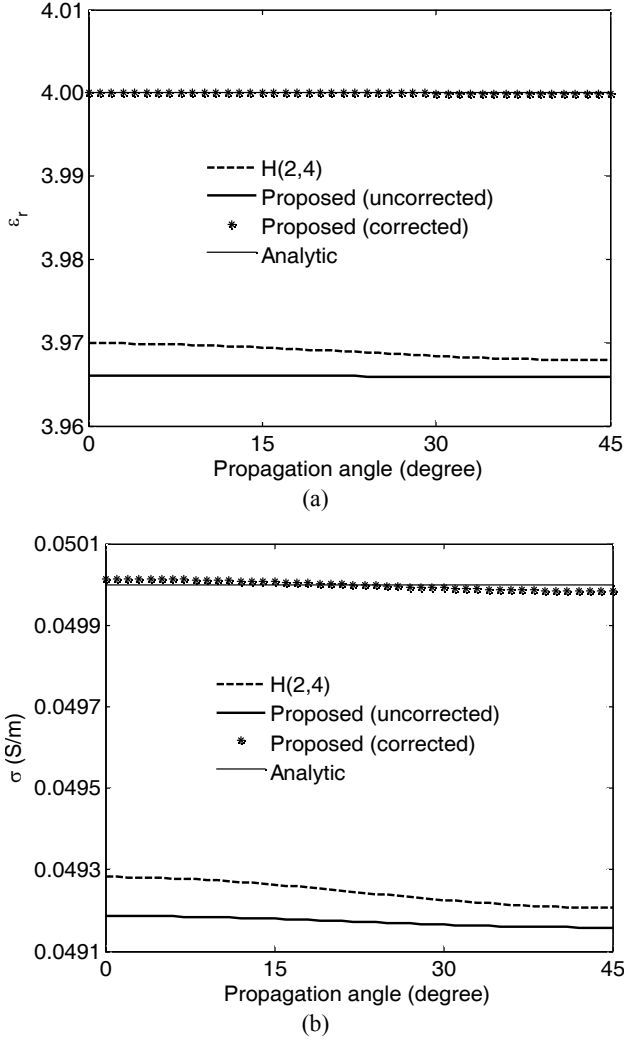


Fig. 5. (a) Relative permittivity and (b) conductivity comparison between the H(2, 4) scheme, proposed scheme, and analytic values. Simulation settings are 10 cells per wavelength and 0.6 S at 10 GHz. S =Courant number.

persion relation. Eq. (15) represents the new numerical dispersion relation.

$$\begin{aligned} & \sin^2\left(\frac{\tilde{k}_x}{2}\right)\left\{1 + \frac{F_w}{6}\sin^2\left(\frac{\tilde{k}_x}{2}\right)\right\}^2 + \sin^2\left(\frac{\tilde{k}_y}{2}\right)\left\{1 + \frac{F_w}{6}\sin^2\left(\frac{\tilde{k}_y}{2}\right)\right\}^2 \\ & = m_1\left(\frac{\Delta}{c\Delta t}\right)^2 \sin^2\left(\frac{\omega\Delta t}{2}\right) - j\frac{m_2\sigma\mu\Delta}{4\Delta t}\sin(\omega\Delta t) \end{aligned} \quad (15)$$

The numerical wavenumber (\tilde{k}) of Eq. (15) is changed into the exact wavenumber (k), thereby allowing analytical calculation of the scaling factors. The solution of Eq. (15) is derived as follows:

$$m_1 = \text{Re}\left[\frac{\sum_{u=x,y}\sin^2\left(\frac{k_u}{2}\right)\left\{1 + \frac{F_w}{6}\sin^2\left(\frac{k_u}{2}\right)\right\}^2}{\left(\frac{\Delta}{c\Delta t}\right)^2 \sin^2\left(\frac{\omega\Delta t}{2}\right)}\right] \quad (16)$$

$$m_2 = -\text{Im}\left[\frac{\sum_{u=x,y}\sin^2\left(\frac{k_u}{2}\right)\left\{1 + \frac{F_w}{6}\sin^2\left(\frac{k_u}{2}\right)\right\}^2}{\frac{\sigma\mu\Delta}{4\Delta t}\sin(\omega\Delta t)}\right] \quad (17)$$

$\text{Re}[X]$ and $\text{Im}[X]$ represent the real and imaginary part of X . The corrected case in Fig. 5 then represents the final performance of the proposed scheme at the operating frequency. The estimated material constants (relative permittivity and conductivity) are almost the same as the analytic values.

The wideband properties of the proposed scheme are analyzed by defining $e_\epsilon(\text{CPW}, S)$ and $e_\sigma(\text{CPW}, S)$ as follows:

$$e_\epsilon(\text{CPW}, S) = \max\left(1 - \frac{\tilde{\epsilon}_r(\phi, \text{CPW}, S)}{\epsilon_r}\right) \quad (18)$$

$$e_\sigma(\text{CPW}, S) = \max\left(1 - \frac{\tilde{\sigma}(\phi, \text{CPW}, S)}{\sigma}\right) \quad (19)$$

where $\tilde{\epsilon}_r$ and $\tilde{\sigma}$ are the estimated relative permittivity and conductivity, respectively. Fig. 6 the proposed scheme

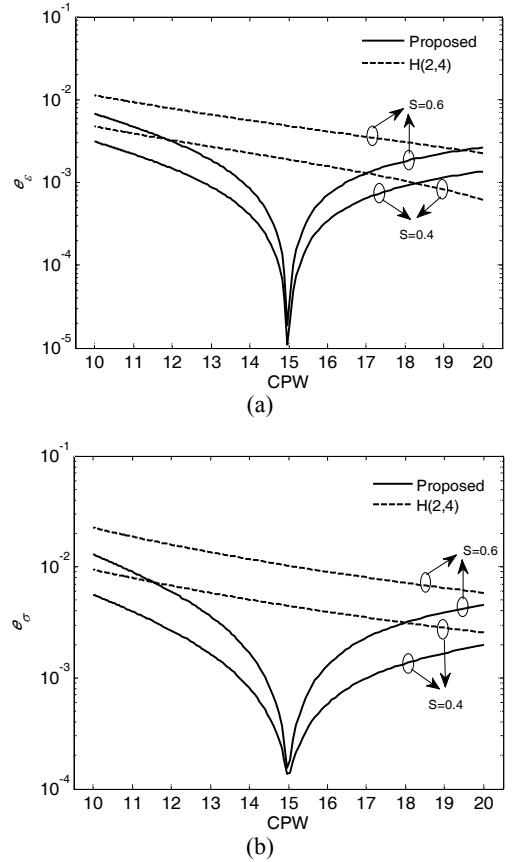


Fig. 6. Error comparison between the proposed and H(2, 4) schemes: (a) e_ϵ and (b) e_σ . The relative permittivity is 4 and the conductivity is 0.05 S/m. S =Courant number.

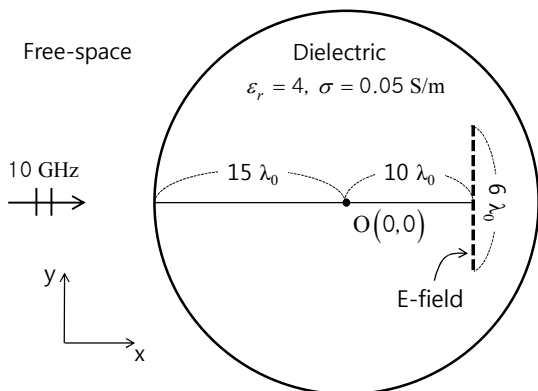


Fig. 7. Calculation settings.

has a much better performance than the H(2, 4) scheme for the wide CPW region. As expected, the proposed scheme has an extremely small error in the selected CPW. In addition, the proposed scheme has similar accuracy for the different Courant numbers in the selected CPW.

IV. Numerical Results

The validity of the proposed scheme for lossy material was verified by calculating a scattering problem of the lossy circular dielectric. The radius of the dielectric is $15 \lambda_0$ at 10 GHz. The dielectric is $\epsilon_r = 4$ and $\sigma = 0.05$ S/m. A single tone plane wave is used as a source. Fig. 7 shows the simulation structure and conditions. The simulation settings are 20 CPW and 0.6 S at 10 GHz. The weighting factor and scaling factors are calculated by Eqs. (9), (16), and (17). The exact solutions were found in [8] and are compared with the calculated results. Fig. 8 shows that the results of the proposed scheme are in better agreement with the analytic solutions than are the results of the H(2,

4) and Yee schemes.

V. Conclusion

In this study, we expanded the optimized H(2, 4) scheme to a lossy material and assumed a square grid. A weighting factor calculated by a closed-form solution was used to obtain isotropic dispersion in the proposed scheme. Two scaling factors were applied to the relative permittivity and conductivity and removed the numerical errors in the optimized CPW. The proposed scheme has better performance than the H(2, 4) scheme with the optimized CPW. The proposed scheme can be used effectively in electrically large problems, and can easily be expanded to 3D.

This work has been supported by the Low Observable Technology Research Center Program of Defense Acquisition Administration and Agency for Defense Development.

References

- [1] J. C. Ju, H. Y. Lee, D. C. Park, and N. S. Chung, "FDTD analysis of lightning-induced voltages on shielded telecommunication cable with multipoint grounding," *Journal of the Korea Electromagnetic Engineering Society*, vol. 1, no. 1, pp. 88-94, May 2001.
- [2] H. J. Kang and J. H. Choi, "Full-wave analysis of microwave amplifiers with nonlinear device by the FDTD algorithm," *Journal of the Korea Electromagnetic Engineering Society*, vol. 2, no. 2, pp. 81-86, Nov. 2002.

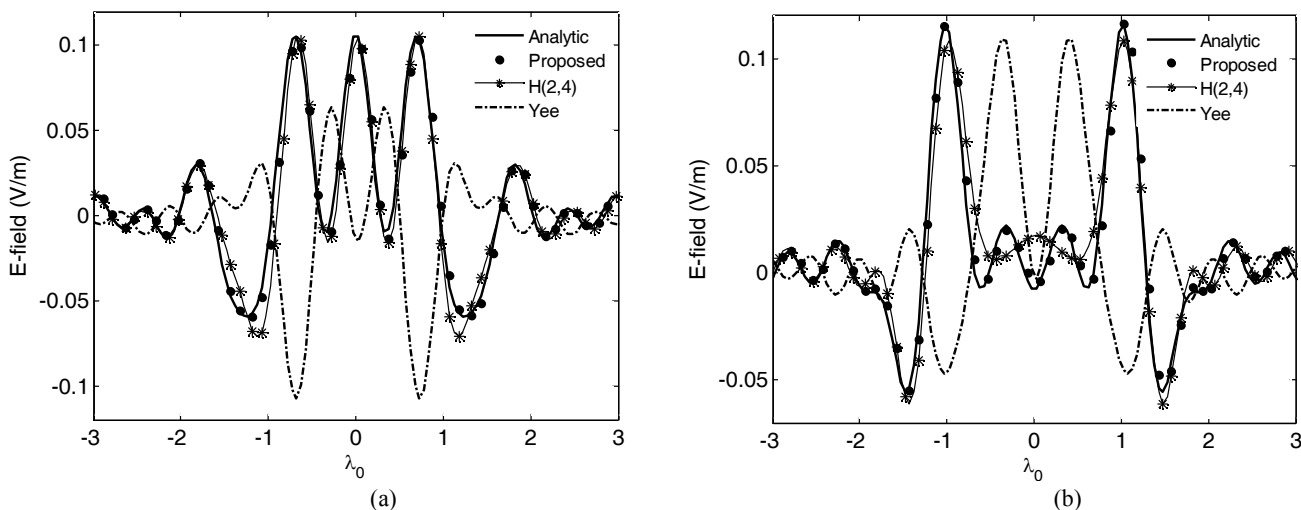


Fig. 8. Comparison of the total E-field of the proposed scheme, the H(2, 4) scheme, and the analytic solution: (a) real parts and (b) imaginary part.

- [3] T. Dogaru and C. Le, "SAR images of rooms and buildings based on FDTD computer models," *IEEE Transactions on Geoscience and Remote Sensing*, vol. 47, no. 5, pp. 1388-1401, May 2009.
- [4] J. B. Wang, B. H. Zhou, B. Chen, L. H. Shi, and C. Gao, "Weakly conditionally stable FDTD method for analysis of 3D periodic structures at oblique incidence," *Electronics Letters*, vol. 48, no. 7, pp. 369-371, Mar. 2012.
- [5] K. Yee, "Numerical solution of initial boundary value problems involving Maxwell's equations in isotropic media," *IEEE Transactions on Antennas Propagation*, vol. 14, no. 3, pp. 302-307, May 1966.
- [6] I. S. Koh, H. Kim, J. M. Lee, J. G. Yook, and P. S. Chang, "Novel explicit 2-D FDTD scheme with isotropic dispersion and enhanced stability," *IEEE Transactions on Antennas Propagation*, vol. 54, no. 11, pp. 3505-3510, Nov. 2006.
- [7] W. T. Kim, "Explicit isotropic-dispersion finite-difference time-domain algorithm, its characteristics and applications," Ph.D. dissertation, Yonsei University, Seoul, Korea, 2010.
- [8] H. Kim, "Explicit and implicit low dispersion FDTD algorithm based on isotropic-dispersion finite difference approximation," Ph.D. dissertation, Yonsei University, Seoul, Korea, 2011.
- [9] W. T. Kim, I. S. Koh, and J. G. Yook, "3D isotropic dispersion (ID)-FDTD algorithm: update equation and characteristics analysis," *IEEE Transactions on Antennas Propagation*, vol. 58, no. 4, pp. 1251-1259, Apr. 2010.
- [10] W. T. Kim, I. S. Koh, and J. G. Yook, "3-D isotropic dispersion FDTD algorithm for rectangular grid," *IEEE Antennas and Wireless Propagation Letters*, vol. 9, pp. 522-525, 2010.
- [11] E. A. Forgy and W. C. Chew, "A time-domain method with isotropic dispersion and increased stability on an overlapped lattice," *IEEE Transactions on Antennas Propagation*, vol. 50, no. 7, pp. 983-996, Jul. 2002.
- [12] J. B. Cole, "A high accuracy FDTD algorithm to solve microwave propagation and scattering problems on a coarse grid," *IEEE Transactions on Microwave Theory and Techniques*, vol. 43, no. 9, pp. 2053-2058, Sep. 1995.
- [13] J. Fang, "Time domain computation for Maxwell's equations," Ph.D. dissertation, University of California at Berkeley, Berkeley, CA, 1989.
- [14] I. Y. Oh, Y. Hong, and J. G. Yook, "Optimization method of higher order (2, 4) FDTD method for low dispersion error," in *Proceedings of the 7th European Conference on Antennas and Propagation*, Gothenburg, Sweden, 2013, pp. 2369-2372.
- [15] A. Taflov, *Computational Electrodynamics: The Finite-Difference Time-Domain Method*. Boston, MA: Artech House, 1995.

Il-Young Oh



received the B.S. degree in electrical and electronic engineering from Yonsei University, Seoul, Korea in 2007, where he is currently pursuing the Ph.D. degree. His main research interests are numerical analysis based on low dispersion finite-difference time-domain (FDTD) method, plasma analysis, and HEMP coupling.

Yongjun Hong



received the B.S. and the Ph.D. degrees in physics from Pohang University of Science and Technology, Pohang, Korea, in 2005 and 2011, respectively. He is currently a Senior Researcher at Agency for Defense Development. His main research interests are in the areas of theoretical/numerical electromagnetic modeling and characterization of microwave/millimeter-wave regime vacuum electronic devices and applications of high power electromagnetic wave. Recently, his research team is developing various vacuum electronic devices and radio frequency integrated circuits (RFIC) for wireless power transmission and active denial technology as well as terahertz video sensor.

Jong-Gwan Yook



(S'89—M'97) was born in Seoul, Korea. He received the B.S. and M.S. degrees in electronics engineering from Yonsei University, Seoul, Korea, in 1987 and 1989, respectively, and the Ph.D. degree from The University of Michigan, Ann Arbor, MI, in 1996. He is currently a Professor with the School of Electrical and Electronic Engineering, Yonsei University. He is also serving IE-EE EMC Society as a Distinguished Lecturer in the year 2012 to 2013. His main research interests are in the areas of theoretical/numerical electromagnetic modeling and characterization of microwave/millimeter-wave circuits and components, design of radio frequency integrated circuits (RFIC) and monolithic microwave integrated-circuit (MMIC), and analysis and optimization of high-frequency high-speed interconnects, including signal/power integrity (EMI/EMC), based on frequency as well as time-domain full-wave methods. Recently, his research team is developing various biosensors, such as carbon nano-tube RF biosensor for nanometer size antigen-antibody detection as well as remote wireless vital signal monitoring sensors.